Available online at www.sciencedirect.com
SCIENCE DIRECT
Catalysis Today 106 (2005) 222–226
CATALYSIS TODAY
www.elsevier.com/locate/cattod

Highly active sulfided CoMo catalyst on nano-structured TiO_2

J. Escobar *, J.A. Toledo, M.A. Cortés, M.L. Mosqueira, V. Pérez, G. Ferrat, E. López-Salinas, E. Torres-García

Prog. de Ing. Molecular y Materiales, Instituto Mexicano del Petróleo, Eje Central Lázaro Cárdenas 152, San Bartolo Atepehuacan, Gustavo A. Madero, 07730, México DF, Mexico

Abstract

High surface area (>300 $m^2\ g^{-1}$) nano-structured TiO_2 oxides (ns-T) were used as CoMo hydrodesulfurization catalyst support. Cylindrical extrudates were impregnated by incipient wetness with Mo (2.8 Mo at. nm^{-2}) and Co (atomic ratio Co/(Co + Mo) = 0.3). Characterization of impregnated precursors was carried out by N_2 physisorption, XRD and atomic absorption and laser-Raman spectroscopies. Sulfided catalysts (400 °C, H_2S/H_2) were studied by X-ray photoelectronic spectroscopy. As indicated by XRD and after various preparation steps (extrusion, Mo and Co impregnation and sulfiding) the nano-structured material was well preserved. XPS analyses showed that Co and Mo dispersion over the ns-T support was much higher than that on alumina. Very high surface S concentration suggested that even ns-T was partially sulfided during catalyst activation. Dibenzothiophene hydrodesulfurization activity (5.73 MPa, 320 °C, *n*-hexadecane as solvent) of CoMo/ns-T was two-fold to that of an alumina-supported commercial CoMo catalyst. The improvement was even more remarkable in intrinsic pseudo kinetic constant basis. No important differences in selectivity over the catalysts supported on either Al_2O_3 or ns-T were observed, where direct desulfurization to biphenyl was favored. Both Mo dispersion and sulfidability were enhanced on the ns-T support where Mo^{4+} fraction was notably increased (~100%) as to that found on $CoMo/Al_2O_3$.

Keywords: Sulfided CoMo; Nano-structured TiO_2; Dibenzothiophene hydrodesulfurization

1. Introduction

In recent years, there has been growing interest in the development of novel materials applicable as supports of catalysts for the hydrotreatment (HDT) of oil-derived feedstocks that could improve the properties of supported Co-Mo or Ni-Mo phases. The driving force of these efforts is the need for reformulated catalysts that could enable the production of fuels of ultra-low hetero-atoms (S, N, O, etc.) content.

For several years TiO_2-supported hydrotreating catalysts have attracted attention because the possibility of obtaining highly active materials [1–3]. However, poor textural properties traditionally found for TiO_2 are a drawback that limit its potential practical applications. Several strategies have been attempted to circumvent these disadvantages. Al_2O_3-TiO_2 [4,5] and ZrO_2-TiO_2 [6,7] mixed oxides have been synthesized offering promising results in both hydrodesulfurization and aromatics hydrogenation reactions.

On the other hand, high surface area anatase titania has been prepared by multi-gelation method [2,8], where the corresponding supported CoMo catalyst showed high activity in light gas oil HDT. In addition, the hydrodenitrogenating function was also improved at low hydrogen consumption.

Recently, we synthesized high surface area (>300 $m^2\ g^{-1}$) nano-structured TiO_2 oxides (ns-T) through a proprietary methodology [9]. Its suitability as CoMo catalyst support is reported in this work. Characterization of impregnated precursors and sulfided catalyst using various techniques was focused on explaining the catalytic activity observed in dibenzothiophene hydrodesulfurization (DBT HDS). The final sulfided catalyst performance is compared to that of a conventional commercial Al_2O_3-supported formulation.

* Corresponding author. Tel.: +52 55 9175 8389; fax: +52 55 9175 8434.
E-mail address: jeaguila@imp.mx (J. Escobar).

0920-5861/$ – see front matter © 2005 Elsevier B.V. All rights reserved.
doi:10.1016/j.cattod.2005.07.136

2. Experimental

2.1. Support preparation

Nano-structured titania powder (ns-T) was prepared as described in [9]. ns-T powder was turned into a paste with 5 wt% citric acid aqueous solution and then it was extruded in a mechanical extruder into cylindrical particles of 1/16 in. (1.59 mm) diameter. Then, the as-made extrudates were dried at 120 °C, (4 h), and annealed at 300 °C (4 h), under dynamic dry air atmosphere. Side crushing strength of extrudates was 6.6 kg mm^{-1} (ASTM D-4179-01 method).

2.2. Mo and Co impregnation

The dried shaped support was impregnated by incipient wetness method at 2.8 Mo at.% nm^{-2} (nominal concentration) with an ammonium heptamolybdate [$(NH_4)_6Mo_7O_{24}\cdot 4H_2O$] solution. The pH of the solution was adjusted to 10.0 by adding NH_4OH. The extrudates were aged (6 h) at ambient conditions then dried at 120 °C (18 h). A $Co(CH_3COO)_2$ aqueous solution was used to reach a Co/(Co + Mo) atomic ratio of 0.3 in the impregnated material, and then they were aged in a closed vessel (6 h). Finally, the impregnated extrudates were dried (120 °C, 18 h) ground and sieved (Tyler mesh 200, ~0.165 mm particle size). The solids were then heat-treated at 400 °C under N_2 (100 ml min^{-1}). After two hours on stream, gas flow was switched to an in situ made H_2S/H_2 mixture (6 ml min^{-1}/50 ml min^{-1}).

2.3. Materials characterization

The textural properties of impregnated materials were studied by N_2 physisorption (at −196 °C), in a Micromeritics ASAP 2000 apparatus. The identity of crystal phases of the solids was examined by X-ray diffraction. Patterns of the samples ($5^\circ < 2\theta < 70^\circ$) packed in a glass holder were recorded at room temperature with Cu Kα radiation (λ = 1.5406 Å) in a Siemens D-500 diffractometer with a graphite secondary beam monochromator. The Cu Kα contribution was eliminated by DIFFRAC/AT software. Ni and Mo content in calcined samples were determined by atomic absorption spectroscopy (Perkin-Elmer 2380). Raman spectra were recorded at room temperature using a Jobin Yvon Inc. Horiba T64000 spectrometer, equipped with a confocal microscope (Olympus, BX41) and a laser beam (514.5 nm) at a power level of 30 mW. Sulfided catalysts (400 °C, 2 h, 30 ml min^{-1} H_2S/H_2 10%, v/v) were analyzed by XPS. The spectra were obtained in a THERMO-VG SCALAB 250 spectrometer equipped with Al Kα X-ray source (1486.6 eV) and a hemispherical analyzer. Experimental peaks were decomposed into components using mixed Gaussian–Lorentzian functions and a non-linear squares fitting algorithm. Shirley background subtraction was applied. An intensity ratio of 2:3 and a splitting of 3.2 eV were used to fit the Mo 3d peaks. Binding energies were reproducible to within ±0.2 eV and the C 1s peak at 284.6 eV was used as a reference from adventitious carbon.

2.4. Activity tests

Sulfided catalysts were tested in DBT HDS in a tri-phase batch reactor (Parr 4575 M), using *n*-hexadecane as solvent. A commercial $CoMo/Al_2O_3$ formulation (CoMo/A, 14.6 wt% Mo, 3.5 wt% Co, 1.87 wt% P, ~5 wt% SiO_2 in the support) was used as reference. Operating conditions (carefully chosen to avoid external and/or internal diffusional limitations) were P = 5.73 MPa, T = 320 °C and 1000 rpm (~105 rad s^{-1}) mixing speed. Samples taken periodically were analyzed in a Varian 3400 CX gas chromatograph (FID detector and dimethylpolysiloxane capillary column, 50 m × 0.2 mm × 0.5 μm). HDS kinetic constants were calculated assuming pseudo-first order kinetics referred to DBT concentration (x = conversion, t = time):

$$k = \frac{-\ln(1-x)}{t} \quad (1)$$

3. Results and discussion

3.1. Materials characterization

Textural properties of the ns-T powder are shown in Table 1. After shaping, the cylindrical extrudates did not show important variations in surface area as to that of the initial powder. On the other hand, pore volume and pore diameter were slightly decreased. The loss in both surface area and pore volume were higher than that originated by the addition of non-porous impregnated phases. Thus, some degree of pore plugging could not be neglected. The impregnated material showed good

Table 1
Textural properties and composition (by atomic absorption spectroscopy, precursors calcined at 300 °C) of the studied materials

Material	Surface area (m^2 g^{-1})	Pore volume (cm^3 g^{-1})	Pore diameter (nm)	Mo (wt%)	Co (wt%)	P (wt%)
ns-T[a]	343	0.70	7.8	–	–	–
ns-T[b]	335	0.47	5.6	–	–	–
CoMo/ns-T[c]	181	0.29	6.3	nd	nd	–
CoMo/ns-T[d]	174	0.29	7.9	12.19	3.43	–
CoMo/A[e]	225	0.50	8.9	14.60	3.50	1.87

nd: not determined.
[a] Dry powder.
[b] Dry cylindrical extrudate.
[c] Impregnated and dried.
[d] Final sulfided catalyst.
[e] Impregnated and calcined.

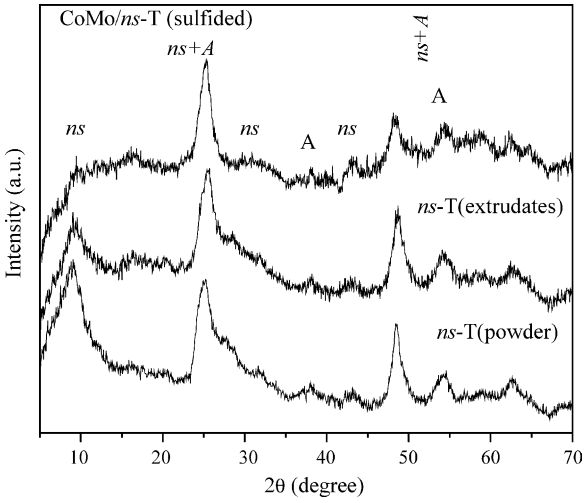

Fig. 1. X-ray diffraction pattern of ns-T and CoMo/ns-T sulfided catalysts.

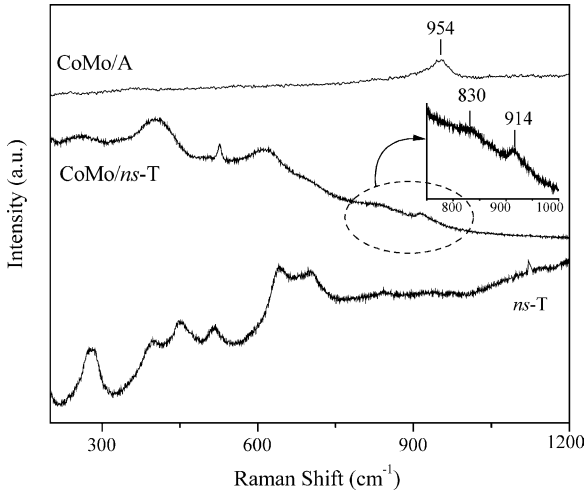

Fig. 2. Raman spectra of ns-T and oxidic CoMo impregnated precursors.

stability during sulfiding as no appreciable variations in texture were registered after catalyst activation. Textural properties of the alumina-supported commercial formulation were included as reference (see Table 1).

Although for the ns-T-supported solid calcining was not included during catalyst preparation Co and Mo contents were determined in the impregnated precursor annealed at 300 °C, to rule out interferences due to residua from the impregnation step. From Table 1, CoMo/ns-T had slightly lower Mo content than CoMo/A.

XRD pattern of the as-synthesized ns-T powder (Fig. 1) showed the characteristic peaks of the nano-structured titania support, which could not be assigned to any known titania structure, like anatase, rutile or brookite [10], although small amounts of poorly crystallized anatase appeared to be embedded in the ns-T matrix. After extrusion, impregnation and sulfiding procedures, ns-T structure was preserved. Notwithstanding, the peak at $2\theta = 9.5^{\circ}$ disappeared after impregnation, probably due to decreased interlayer distance in the ns-T material [11].

Raman spectrum of the support showed six broad bands at 280, 397, 450, 515, 640 and 700 cm^{-1} (see Fig. 2). Accordingly, the bands at 397, 515 could be assigned to the anatase phase of TiO_2 [12] while the three bands at 280, 450 and 700 cm^{-1} were related to vibrating modes of ns-T [13]. The signal at 640 cm^{-1} could be related to either of those two phases. These results corroborated that the support was composed of anatase and ns-T phases. After impregnation and calcining (at 300 °C), the Raman spectrum showed broad bands at 260, 400 and 615 cm^{-1}, which correspond to those of ns-T support, although shifted to lower energies possibly due to weakening of the related Ti–O bonds. Raman spectrum of the commercial reference Co-Mo/A showed only a broad peak centered at 954 cm^{-1}, which has been assigned to terminal Mo=O stretching modes [14] in octahedral environment. In our CoMo/ns-T sample, two broad bands were observed (inset of Fig. 2) one centered at 914 cm^{-1} and the other at 830 cm^{-1}, which have been assigned to symmetrical and asymmetrical stretching modes of terminal Mo=O in tetrahedral environment (MoO_4^{2-}) [14]. The presence of this species could be explained by considering that the impregnation was made under strong basic conditions (pH 10) where MoO_4^{2-} anions are predominant [2]. The tetrahedral environment of these well dispersed Mo species remained after annealing at 300 °C.

Another sharp band at 527 cm^{-1} was observed for the CoMo/ns-T sample. This peak that was not detected in the commercial Co-Mo/A catalyst, could be assigned to Mo–O–Co vibrating modes. This signal has been reported [15] to appear in the 540–580 cm^{-1} range in heteropolymolybdate structures. In our case, the observed shift to lower frequencies suggested a strong interaction between cobalt and molybdenum oxides that could, as a result, weaken their interaction with the support. This could favor a higher sulfiding degree during catalyst activation.

Surface characterization by XPS (Table 2) showed that Co and Mo dispersion over the ns-T was much higher than that on alumina. Very high surface S concentration on CoMo/ns-T suggested that, in addition to supported Co and Mo phases, the nano-strutured material was also partially sulfided during treatment under H_2S/H_2 (400 °C), as previously reported in the case of TiO_2-supported Mo catalysts [3]. Mo dispersion was enhanced (by a factor of ~2) on ns-T, compared to that of CoMo/A. The

Table 2
Surface composition (by XPS) of the sulfided CoMo catalysts studied

Catalyst	S (at.%)	Ti (at.%)	Al (at.%)	Co (at.%)	Mo^{4+} (at.%)	Mo^{5+} (at.%)	Mo^{6+} (at.%)	Co/(Co + Mo) surface ratio
CoMo/ns-T	22.93	10.12	–	3.15	2.36	0.67	0.21	0.49
CoMo/A	4.28	–	20.98	0.73	0.78	0.93	0.52	0.25

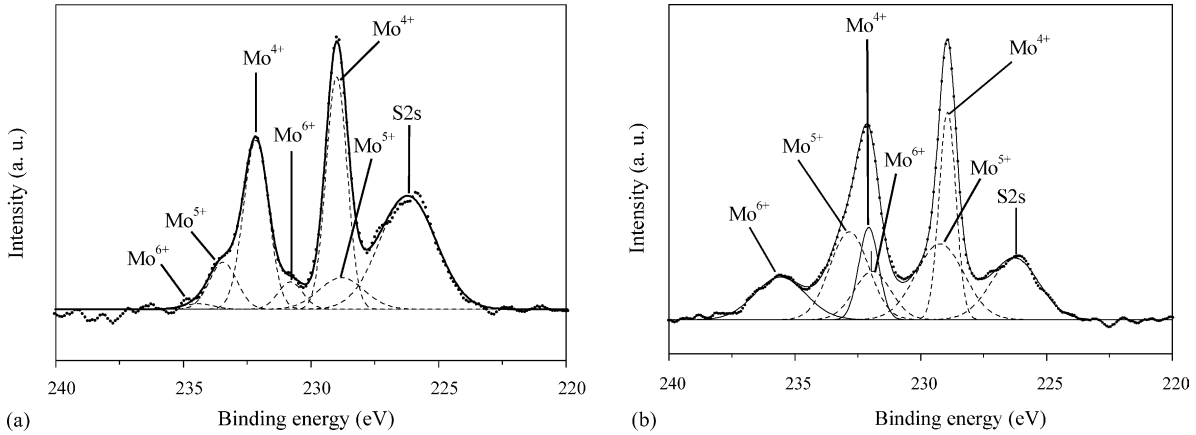

Fig. 3. XPS spectra of catalysts sulfided at 400 °C (2 h, H_2S/H_2) (a) CoMo/ns-T and (b) CoMo/A.

corresponding Mo 3d doublet (Fig. 3a) could be satisfactorily fitted by considering Mo^{4+} (from MoS_2), Mo^{5+} (from molybdenum oxy-sulfides) and Mo^{6+} (unreduced molybdenum) [7]. From total surface Mo measurement, the Mo^{4+} fraction was increased by a factor of two on ns-T, as compared to that found in the commercial reference (Fig. 3b and Table 2). Conversely to that observed on alumina-supported catalysts, tetrahedral MoO_4^{2-} species on ns-T (see Fig. 2) were extensively sulfided at 400 °C. Tetrahedral Mo species in $CoMo/Al_2O_3$ have been associated to refractory $Al_2(MoO_4)_3$ sulfidable at very severe conditions [16]; in contrast, the interaction between ns-T and highly dispersed tetrahedrally coordinated anions seemed to be much weaker allowing to obtain a high sulfiding degree at moderate conditions (Fig. 3a).

The observed Co/(Co + Mo) surface ratio suggested that a higher amount of the so called ''CoMoS'' phase could be present on the nano-structured support. This could result in a high promotion degree of the sulfided Mo by Co.

3.2. Activity test

HDS activity of CoMo/ns-T was twice as to that of the alumina-supported reference (Table 3). This improvement was even more remarkable in intrinsic pseudo kinetic constant (k') basis. No important differences in selectivity between the two catalysts were observed, where direct desulfurization to biphenyl [17] was favored. The small proportion of hydrogenated products (cylohexylbenzene and bicyclohexyl) observed suggested that on our ns-T material Mo could be efficiently promoted by Co [18], in contrast with that reported for anatase TiO_2-supported CoMo catalysts [4].

High dispersion of Co and Mo and their high sulfidability on CoMo/ns-T may be responsible for its remarkable HDS behavior. Our nano-structured ns-T material constitutes a very promising support for the preparation of highly active deep-desulfurization catalysts.

Table 3
Pseudo-first order kinetic constants (k, per mass of catalysts and k', per mass of Mo) in DBT-HDS

Catalyst	$k \times 10^{-4}$ ($m^3\,kg_{cat}^{-1}\,s^{-1}$)	$k' \times 10^{-4}$ ($m^3\,kg_{Mo}^{-1}\,s^{-1}$)
CoMo/ns-T	2.36	19.88
CoMo/A	1.14	7.81

P = 5.73 MPa, T = 320 °C, 1000 rpm mixing speed, solvent: hexadecane.

4. Conclusions

High surface area nano-structured Ti oxide (ns-T) constitutes a very efficient hydrodesulfurization catalyst support. The nano-structured material was well preserved during various catalyst synthesis steps (extrusion, impregnation and sulfiding), although ns-T was partially sulfided during catalyst activation. Dibenzothiophene hydrodesulfurization over CoMo/ns-T was much higher (approximately two-fold) than that on an alumina-supported commercial CoMo catalyst. Negligible differences in selectivity over the catalysts supported in either Al_2O_3 or ns-T were noted, where direct desulfurization to biphenyl was favored, suggesting that in both cases Mo was efficiently promoted by Co. High Mo and Co dispersion and enhanced Mo sulfidability (Mo^{4+} fraction two-fold to that on $CoMo/Al_2O_3$) seemed to determine the activity trends found.

Acknowledgement

The authors acknowledge financial support from IMP (D.00207 and D.00237 grants).

References

[1] S.K. Maity, M.S. Rana, K.S. Bej, J. Ancheyta, G. Murali Dhar, T.S.R. Prasada Rao, Appl. Catal. A 205 (2001) 215.
[2] S. Dzwigaj, C. Louis, M. Breysse, M. Cattenot, V. Belliere, C. Geantet, M. Vrinat, P. Blanchard, E. Payen, S. Inoue, H. Kudo, Y. Yoshimura, Appl. Catal. B 41 (2003) 181.

[3] J. Ramírez, L. Cedeño, G. Busca, J. Catal. 184 (1999) 59.
[4] J. Ramírez, L. Ruiz, L. Cedeño, V. Harlé, M. Vrinat, M. Breysse, Appl. Catal. 93 (1993) 163.
[5] J.R. Grzechowiak, I. Wereszczako-Zielińska, K. Rynkowski, M. Zió-łek, Appl. Catal. A 250 (2003) 95.
[6] C.-M. Lu, Y.-M. Lin, I. Wang, Appl. Catal. A 198 (2000) 223.
[7] M. Barrera, M. Viniegra, J. Escobar, M. Vrinat, J.A. De Los Reyes, F. Murrieta, J. García, Catal. Today 98 (2004) 131.
[8] S. Inoue, A. Muto, H. Kudou, T. Ono, Appl. Catal. A 269 (2004) 7.
[9] J.A. Toledo, J. Escobar, M.A. Cortés, M.L. Mosqueira, V. Pérez, C. Angeles, E. López-Salinas, M. Lozada, Patent PCT/MX2003/00081 (2005).
[10] X. Bokhimi, A. Morales, M. Aguilar, J.A. Toledo, F. Pedraza, Int. J. Hydrogen Energy 26 (2001) 1279.
[11] A. Clearfield, J. Lehto, J. Solid State Chem. 73 (1988) 98.
[12] U. Balachandran, N.G. Eror, J. Solid State Chem. 42 (1982) 276.
[13] R. Ma, K. Fukuda, T. Sasaki, M. Osada, Y. Bando, J. Phys. Chem. B 109 (2005) 6210.
[14] J.A. Bergwerff, T. Visser, B.R.G. Leliveld, B.D. Rossenaar, K.P. de Jong, B.M. Weckhuysen, J. Am. Chem. Soc. 126 (2004) 14548.
[15] C. Martin, C. Lamonier, M. Fournier, O. Mentré, V. Harlé, D. Guillaume, E. Payen, Inorg. Chem. 43 (2004) 4636.
[16] Z. Wei, Sh. Jiang, Q. Xin, Sh. Sheng, G. Xieng, Catal. Lett. 11 (1991) 365.
[17] M. Houalla, N.K. Nag, A.V. Sapre, D.H. Broderick, B.C. Gates, AIChE J. 24 (1978) 1015.
[18] F. Bataille, J.L. Lemberton, G. Pérot, P. Leyrit, T. Cseri, N. Marchal, S. Kasztelan, Appl. Catal. A 220 (2001) 191.